Control of quantum dynamics by optimized measurements

Feng Shuang,[1] Mianlai Zhou,[2] Alexander Pechen,[1]
Rebing Wu,[1] Ofer M. Shir,[1,3] and Herschel Rabitz[1]

[1]*Department of Chemistry, Princeton University, Princeton, New Jersey 08544*
[2]*National Laboratory for Physical Sciences at Micro Scale,*
University of Science and Technology of China, Hefei, China
[3]*Natural Computing Group, Leiden University, Leiden, Netherlands*

(Dated: February 16, 2009)

Abstract

Quantum measurements are considered for optimal control of quantum dynamics with instantaneous and continuous observations utilized to manipulate population transfer. With an optimal set of measurements, the highest yield in a two-level system can be obtained. The analytical solution is given for the problem of population transfer by measurement-assisted coherent control in a three-level system with a dynamical symmetry. The anti-Zeno effect is recovered in the controlled processes. The demonstrations in the paper show that suitable observations can be powerful tools in the manipulation of quantum dynamics.

I. INTRODUCTION

Control of quantum processes has attracted considerable attention, both theoretically [1, 2, 3, 4, 5, 6] and experimentally [7, 8, 9]. Most studies of quantum control are concerned with shaping a laser pulse to achieve an expected goal. However, a coherent laser pulse is not the only driving force for quantum dynamics. Incoherent driving forces, such as laser noise, decoherence from the environment, and quantum observations, can also influence quantum dynamics. A natural general expectation is that the later influence will be deleterious toward achieving control [10]. However, recent studies [11, 12] have shown that controlled quantum dynamics can survive intense field noise and decoherence, as well as even cooperate with them under special circumstances [13]. Under these special conditions, it is possible to meet the target goal more effectively with the help of laser noise and environmental decoherence. Incoherent non-unitary control of quantum systems by a suitably optimized environment (e.g., incoherent radiation, a gas or solvent, a cloud of electrons, atoms or molecules, etc.) was suggested as a supplement to coherent control to provide a general tool for selective manipulation of both the Hamiltonian and dissipative aspects of the system dynamics [14, 15].

Both the outcome and back-action from quantum measurements could be used to control quantum processes. In standard closed-loop optimal control [16], the quantum system is non-selectively measured when the desired evolution ends, and the outcomes of the measurements are used by a learning algorithm to optimize the laser pulse. Measurements were also used to map an unknown mixed state onto a known target pure state [17]. Some investigations considered exploiting the back action from the quantum observations, and control by measurement plus dynamical evolution was proposed [18]. The control of the population branching ratio between two degenerate states by continuous measurements was treated [19], and the effect of nonoptimized measurements on control by lasers was investigated [20, 21].

Numerical simulations have been performed to investigate observations serving as indirect controls in the manipulation of quantum dynamics [22]. Optimal control fields were shown to be capable of cooperating or fighting with observations to achieve a good yield, and the nature of the observations may be optimized to more effectively control the quantum dynamics. Quantum observations also can break dynamical symmetries to increase the controllability of a quantum system. The quantum Zeno and anti-Zeno effects induced by

observations are the key operating principles in these processes. When instantaneous observations are the only forces to drive population transfer in a two-level system, the maximal population transfer induced by a finite number of measurements has been found, and the quantum anti-Zeno effect is recovered in the limit of infinitely frequent measurements [23].

In this paper, we further explore the utility of quantum measurements as controls in the manipulation of quantum dynamics. Here we assume that any projection operator may be observed in a suitably performed experiment. Analytical solutions and upper bounds of several controlled processes are found. The remainder of the paper is organized as follows: Section II reviews the main concepts of instantaneous and continuous measurements, which are used as controls in this paper. The analytical solutions for instantaneous and continuous observations in a two-level system are explored in Sec. III and IV, respectively. The maximal measurement-assisted population transfer in a system with dynamical symmetry is obtained in section V. A brief summary is presented in section VI.

II. QUANTUM OBSERVATIONS

Quantum measurement serves as an incoherent driving force, and there are two general types of quantum measurements: instantaneous von Neumann measurements and continuous measurements. A characteristic feature of quantum systems is that their measurement unavoidably affects the associated dynamics. The well known manifestation of this back reaction is the uncertainty principle [24]. The influence of a measurement is revealed in a more direct way through a change of the measured system state. In von Neumann axiomatic quantum mechanics it is postulated that any measurement gives rise to an abrupt change of the state of the system (instantaneous measurements) under consideration and projects it onto an eigenstate of the measured observable [25]. The measurement process follows irreversible dynamics, and causes the disappearance of coherence of the system's state: the off-diagonal elements of the density matrix decay, or the phases of the wavefunction amplitudes are randomized. Density matrices are adopted to describe the states of controlled systems, because the nonselective quantum measurements in the paper are applied to an ensemble of quantum systems.

A. Instantaneous measurements

An ideal measurement occurs at one instant of time or a sequence of such observations may be performed at different instants [25]. Let $Q = \sum_i q_i P_i$ be an observable with q_i being the eigenvalue of P_i, which is a projector such that $P_i P_j = P_i \delta_{ij}$ and $\sum_i P_i = 1$. The measurement of Q converts the state ρ of the system just before the measurement into the state

$$\rho' \equiv \mu_Q(\rho) = \sum_k P_k \rho P_k. \tag{1}$$

A projection operator P satisfies $P = P^2$, and its spectral decomposition may be written as $P = q_0 P_0 + q_1 P_1$ with the two eigenvalues being $q_0 = 0$ and $q_1 = 1$ and two corresponding projectors being $P_0 = 1 - P$ and $P_1 = P$. Thus, according to Eq. (1), observation of the operator $Q = P$ transforms the density matrix ρ of the system into ρ' given by

$$\rho' = \mu_P(\rho) = P_0 \rho P_0 + P_1 \rho P_1 \tag{2a}$$

$$= \rho - [P, [P, \rho]], \tag{2b}$$

so $[P, [P, \rho]]$ is the "kick" by an instantaneous observation of the projection operator P.

B. Continuous measurements

There are two equivalent theoretical formulations of continuous quantum measurements [26]. One of them is based on restricted path integrals (RPI) and the other one on master equations (ME). For simplicity, we adopt the latter formulation. Corresponding to a continuous measurement of a single observable, the master equation has the form [27]:

$$\dot{\rho} = -i[H, \rho] - \frac{1}{2}\kappa [A, [A, \rho]]. \tag{3}$$

Here, H is the Hamiltonian of the measured system, A is the measured operator. Equation (3) is similar with the equation describing a system interacting with the environment, so we could call κ as the "strength" of the observation.

C. Quantum ZENO and Anti-ZENO Effect

Prevention of a quantum system's time evolution by means of repetitive, frequent observations or continuous observations of the system's state is the quantum Zeno effect (QZE). The

QZE was proposed by Misra and Sudarshan [28] and was experimentally demonstrated [29] in a repeatedly measured two-level system undergoing Rabi oscillations. A time-dependent observable projection operator inducing up to 100% transfer from one state to another state [30] is the quantum anti-Zeno effect (QAZE). The impacts of QZE and QAZE operations are the key processes explored in this paper to help control quantum dynamics.

III. TWO-LEVEL SYSTEM CONTROLLED BY INSTANTANEOUS MEASUREMENTS

This section presents the analytical solution for the control of population transfer in a two-level system by optimized instantaneous measurements. The objective is to drive the population from the initial state $\rho_0 = |0\rangle\langle 0|$ to the final state $\rho_f = |1\rangle\langle 1|$. An observable Q has the form $Q = q_1 P_1^{(Q)} + q_2 P_2^{(Q)}$, where q_1 and q_2 its the eigenvalues, and $P_1^{(Q)}$ and $P_2^{(Q)}$ are the corresponding projectors. From Eq. (2), it's easy to see that the measurement of Q is equal to the measurement of the projector $P_1^{(Q)}$, since $P_2^{(Q)} = 1 - P_1^{(Q)}$. Thus, it is sufficient to consider the measurement of projection operators in this case.

A sequence of N instantaneous projection observations, specified by the operators

$$P_k = |\psi_k\rangle\langle\psi_k|, \tag{4a}$$

$$|\psi_k\rangle = \cos\frac{\alpha_k}{2}|0\rangle + e^{i\theta_k}\sin\frac{\alpha_k}{2}|1\rangle. \tag{4b}$$

are performed at times T_k, $k = 1, \cdots, N$. Parameters α_k and θ_k in Eq. (4b) are limited to the range

$$-\frac{\pi}{2} \le \frac{\alpha_k}{2} < \frac{\pi}{2}, \tag{5a}$$

$$0 \le \theta_k < \pi, \tag{5b}$$

since the projection operator P_k does not depend on the phase of $|\psi_k\rangle$. The operators P_k parameterized by α_k and θ_k, $k = 1, \cdots, N$, are optimized to maximize the yield,

$$Y_N[P_1, \cdots, P_N] = \langle 1|\rho_N|1\rangle. \tag{6}$$

Here ρ_N is the density matrix after performance of N observations given by the iterative equation

$$\rho_k = \rho_{k-1} - [P_k, [P_k, \rho_{k-1}]], \qquad k = 1, \cdots, N \tag{7}$$

with $\rho_0 = |0\rangle\langle 0|$ and P_k described in Eq. (4a). We have neglected the free evolution between measurements, which is easy to include via a transformation between the Schrödinger picture and interaction picture,

$$\rho_k = e^{iH_0T_k}\rho_k^{(S)}e^{-iH_0T_k}, \tag{8a}$$

$$P_k = e^{iH_0T_k}P_k^{(S)}e^{-iH_0T_k}. \tag{8b}$$

Here $\rho_k^{(S)}$ is the density matrix in the Schrödinger picture governed by the iterative equation,

$$\rho_k^{(S)} = e^{-iH_0(T_k-T_{k-1})}\{\rho_{k-1}^{(S)} - [P_k^{(S)},[P_k^{(S)},\rho_{k-1}^{(S)}]]\}e^{iH_0(T_k-T_{k-1})}, k = 1,\cdots,N, \tag{9}$$

which includes the free evolution.

The density matrix ρ_N is Hermitian with unit trace. Hence, it can be expressed in the for

$$\rho_N = \begin{pmatrix} 1-Y_N & Z_N^* \\ Z_N & Y_N \end{pmatrix}. \tag{10}$$

It is easy to establish the following solution to the iteration in Eq. (7)

$$Y_k = \langle 1|\,\rho_k\,|1\rangle = \frac{1}{2}\left(1-\cos\alpha_1 C_{12}C_{23}\cdots C_{k-1,k}\cos\alpha_k\right), \tag{11a}$$

$$Z_k = \langle 1|\,\rho_k\,|0\rangle = \frac{1}{2}e^{i\theta_k}\cos\alpha_1 C_{12}C_{23}\cdots C_{k-1,k}\sin\alpha_k, \tag{11b}$$

with the coefficients C_{mn} given by

$$C_{mn} = \cos\alpha_m\cos\alpha_n + \cos\left(\theta_m-\theta_n\right)\sin\alpha_m\sin\alpha_n. \tag{12}$$

Therefore,

$$Y_N = \frac{1}{2}\left(1-\cos\alpha_1 C_{12}C_{23}\cdots C_{N-1,N}\cos\alpha_N\right) \tag{13}$$

is the yield from N observations.

We will now determine the maximum value of Y_N, which is a function of variables θ_k and α_k. The inequality (5b) yields $-\pi < \theta_m - \theta_n < \pi$ and $1 \geq \cos\left(\theta_m-\theta_n\right) > -1$. Setting to zero the derivative of Y_N with respect to θ_k gives $\sin\left(\theta_k-\theta_{k-1}\right) = 0$ for $k = 2,\cdots,N$. Hence Y_N reaches its maximum when

$$\theta_1 = \theta_2 = \cdots = \theta_N \tag{14}$$

Therefore, after optimization with respect to θ_k, Y_N can be written as an function of α_k, $k = 1, \cdots, N$,

$$Y_N^{(\alpha)} = \frac{1}{2}\left[1 - \cos\alpha_1 \cos\left(\alpha_1 - \alpha_2\right) \cdots \cos\left(\alpha_{N-1} - \alpha_N\right) \cos\alpha_N\right] \tag{15a}$$

$$= \frac{1}{2}\left[1 + \prod\nolimits_{k=0}^{N} \cos\varphi_k\right], \tag{15b}$$

with $\varphi_0 = \pi - \alpha_1$, $\varphi_1 = \alpha_1 - \alpha_2$, $\cdots$, $\varphi_{N-1} = \alpha_{N-1} - \alpha_N$ and $\varphi_N = \alpha_N$. It is easy to verify that the second derivative of the function $f(x) = \ln\cos(x)$ is negative, so it is a concave function. The inequality,

$$\prod\nolimits_{k=0}^{N} \cos\varphi_k \leq \left(\cos\frac{\pi}{N+1}\right)^N, \tag{16}$$

can be established by the majorization inequality [31] for concave functions,

$$\frac{\sum_{k=1}^{M} f(x_k)}{M} \leq f\left(\frac{\sum_{k=1}^{M} x_k}{M}\right). \tag{17}$$

Hence, $Y_N^{(\alpha)}$ reaches its maximum value

$$Y_N^{(O)} = \frac{1}{2}\left[1 + \left(\cos\frac{\pi}{N+1}\right)^{N+1}\right], \tag{18}$$

when $\varphi_0 = \cdots = \varphi_N = \frac{\pi}{N+1}$. The solutions are consistent with what was found in [23]. The QAZE is recovered in the limit of an infinite number of observations,

$$\lim_{N\to\infty} Y_N^{(O)} = 1. \tag{19}$$

IV. TWO-LEVEL SYSTEM CONTROLLED BY CONTINUOUS MEASUREMENTS

In this section, the quantum dynamics of a two-level system is controlled by suitable continuous measurements. Here we assume that it is possible to continuously measure any time-dependent projection operator $P(t)$. In the interaction picture, the dynamics of the continuous observation process is described by

$$\dot{\rho}(t) = -\gamma\mathcal{L}(t)\rho(t) = -\gamma\left[P(t), \left[P(t), \rho(t)\right]\right], \tag{20}$$

where $\mathcal{L}(t)$ is a super-operator acting on the density matrix $\rho(t)$, and γ is the constant strength of the observation. The projection operator $P(t)$ is specified by

$$P(t) = |\psi(t)\rangle \langle\psi(t)|, \tag{21a}$$

$$|\psi(t)\rangle = \cos\frac{\alpha(t)}{2}|0\rangle + e^{i\theta(t)}\sin\frac{\alpha(t)}{2}|1\rangle, \tag{21b}$$

where $\alpha(t)$, $\theta(t)$ are functions of time t to be determined. The goal is to optimize the objective functional, as the yield at final time T_f,

$$Y(T_f)[P(t)] = Y(T_f)[\alpha(t), \theta(t)] = \langle 1|\rho(T_f)|1\rangle, \tag{22}$$

where the system is initially populated on state $|0\rangle$.

Eq. (20) appears insoluble for general functions of $\alpha(t)$ and $\theta(t)$. First consider only a simple case, with zero phase and $\alpha(t)$ taken as linear in time,

$$\alpha(t) = A\frac{t}{T_f} + B \tag{23a}$$

$$\theta(t) = 0. \tag{23b}$$

The final yield of this case may be explicitly worked out as

$$Y(T_f) = \frac{1}{2} - \frac{1}{2}e^{-\gamma'}\left\{\cos A\cosh\delta + [\gamma'\cos(2B+A) + A\sin A]\frac{\sinh\delta}{\delta}\right\}, \tag{24}$$

where γ' and δ are dimensionless parameters defined by

$$\gamma' = \frac{1}{2}\gamma T_f \tag{25a}$$

$$\delta = \sqrt{\gamma'^2 - A^2}. \tag{25b}$$

Eq. (24) reaches its maximum value when

$$2B_m + A_m = \pi \tag{26a}$$

$$\gamma'\sin A_m = A_m, \tag{26b}$$

in which case the optimal value of the yield is

$$Y^{(O)}(T_f) = \frac{1}{2}\left(1 - e^{-\gamma'(1+\cos A_m)}\cos A_m\right). \tag{27}$$

Figure 1 depicts the variation of the optimal A_m and B_m with respect to γ', and we conclude that

$$A_m = 0, \text{ for } \gamma' < 1 \tag{28a}$$

$$A_m \to \pi, \text{ for } \gamma' \to \infty. \tag{28b}$$

It follows from Eq. (27) that a complete population transfer is attained when γ' in Eq. (25a) approaches infinity. Thus, from Eq. (25a), increasing the observation strength γ and the final time are equally effective in enhancing the control process, and the QAZE is recovered in the limit of infinite observation strength, or final time.

We now assess whether the linear solution in Eq. (23) is optimal with respect to all possible forms of $\alpha(t)$ and $\theta(t)$. To verify that this is the case, we start from Eq. (20) and consider the variation of $\rho(t)$ with respect to $\alpha(t)$ and $\theta(t)$. The general variation of Eq. (20) gives

$$\frac{d[\delta\rho(t)]}{dt} = -\gamma\left[\mathcal{L}(t)\,\delta\rho(t) + \delta\mathcal{L}(t)\,\rho(t)\right]. \tag{29}$$

and for a driving variation $\delta\alpha(t)$, it is easy to verify that the solution of the above equation is

$$\delta\rho(t) = -\gamma\int_0^t \left[\rho_\alpha(t,\tau)\right]\delta\alpha(\tau)\,d\tau, \tag{30a}$$

$$\rho_\alpha(t,\tau) = \mathcal{U}(t,\tau)\left[\frac{d\mathcal{L}(\tau)}{d\alpha}\rho(\tau)\right], \tag{30b}$$

where $\mathcal{U}(T,t)$ is a time-ordered exponential

$$\mathcal{U}(t,\tau) = \exp_+\left[-\gamma\int_\tau^t \mathcal{L}(\nu)\,d\nu\right]. \tag{31}$$

Hence $\rho_\alpha(t,\tau)$ is the solution of the differential equation

$$\frac{\partial\rho_\alpha(t,\tau)}{\partial t} = -\gamma\mathcal{L}(t)\,\rho_\alpha(t,\tau) \tag{32}$$

with the initial condition

$$\rho_\alpha(\tau,\tau) = \frac{d\mathcal{L}(\tau)}{d\alpha}\rho(\tau). \tag{33}$$

It is evident that $\rho_\alpha(t,\tau)$ is real, symmetric and traceless under the assumption of Eq. (23), hence we can set

$$\rho_\alpha(t,\tau) = \begin{pmatrix} -Y_\alpha(t,\tau) & Z_\alpha(t,\tau) \\ Z_\alpha(t,\tau) & Y_\alpha(t,\tau) \end{pmatrix}. \tag{34}$$

It is easy to yield the result

$$Y_{\alpha}\left(t,\tau\right)=-\frac{1}{2}\sin A\left(1-\frac{t}{T_{f}}\right)\exp\left[\frac{A\left(t-2\tau\right)\cot A-t\csc A}{T_{f}}\right]. \tag{35}$$

So the variation of the final yield with respect to $\alpha\left(t\right)$ is zero,

$$\delta Y^{(O)}\left(T_{f}\right)=-\gamma\int_{0}^{T_{f}}Y_{\alpha}\left(T_{f},\tau\right)\delta\alpha\left(\tau\right)dt=0. \tag{36}$$

Using the same procedures taken above, we can prove that the variation of the final yield with respect to the phase function $\theta\left(t\right)$ is also zero. Hence, the linear solution is an optimal solution.

In addition to the analysis above, we performed numerical simulations, where the goal was optimization of the yield Y by means of an evolutionary algorithm approach to determine $\alpha(t)$ and $\theta(t)$. The optimization procedure was conducted freely, without any preliminary assumptions on $\alpha(t)$ or $\theta(t)$, and without any constraints on their values during the search. For this purpose, we applied the covariance matrix adaptation evolution strategy (CMA-ES) [32, 33] to the task. The latter algorithm is very efficient for treating continuous global optimization problems [34, 35]. It has been successful for handling correlations among object variables. Fig. 2 depicts the best yield from performing full optimization with respect to $\alpha\left(t\right)$ and $\theta\left(t\right)$, when the assumptions in Eq. (23) are not applied. It can be concluded that the solution is globally optimal.

The best yield from continuous measurements, Eq. (27), seems very different to the best yield from instantaneous measurements, Eq. (18). However, their asymptotic forms,

$$Y_{N}^{(O)}\sim1-\frac{\pi^{2}}{4N}, \quad N\rightarrow\infty, \tag{37a}$$

$$Y^{(O)}\left(T_{f}\right)\sim1-\frac{\pi^{2}}{2\gamma T_{f}},\ \gamma T_{f}\rightarrow\infty, \tag{37b}$$

are very similar. Hence the best yield from continuous measurements with measurement strength γ is very close to the best yield from a sequence of $N\simeq\gamma T_{f}/2$ instantaneous measurements, when $\gamma T_{f}\gg1$.

V. OPTIMAL POPULATION TRANSFER IN A SYSTEM WITH DYNAMICAL SYMMETRY BY MEASUREMENT-ASSISTED COHERENT CONTROL

In this section we consider a system whose free Hamiltonian H_0 and dipole moment μ are given by

$$H_0 = \begin{pmatrix} 1 & 0 & 0 \\ 0 & 2 & 0 \\ 0 & 0 & 3 \end{pmatrix}, \qquad \mu = \begin{pmatrix} 0 & 1 & 0 \\ 1 & 0 & 1 \\ 0 & 1 & 0 \end{pmatrix}.$$

The system is initially prepared in the ground state $|\psi_0\rangle = |0\rangle$ at $t = 0$. The control goal is to transfer as much as possible of the population from the ground state $|0\rangle$ to the first excited state $|1\rangle$ at the target time $T > 0$ using as controls a coherent electromagnetic field $\varepsilon(t)$ during the time period $[0, T]$ and a single measurement of the projector $P_0 = |0\rangle\langle 0|$ (or $P_2 = |2\rangle\langle 2|$) at a time $t_1 \in (0, T)$.

The symmetry of the system implies (see Ref. [36]) that the coefficients of a pure system state $|\psi_t\rangle = C_0(t)|0\rangle + C_1(t)|1\rangle + C_2(t)|2\rangle$ satisfy the following relation upon evolution under only the action of a coherent field,

$$\left| C_0(t)C_2(t) - \frac{C_1^2(t)}{2} \right| = \left| C_0(0)C_2(0) - \frac{C_1^2(0)}{2} \right|, \quad \text{for any } t \geq 0. \tag{38}$$

If the initial state is $|\psi_0\rangle = |0\rangle$, then $C_1(0) = C_2(0) = 0$ and Eq. (38) becomes the following relation for the coefficients $C_i(t)$:

$$C_1^2(t) = 2C_0(t)C_2(t)\ , \quad \text{for any } t \geq 0. \tag{39}$$

This relation was used in [22] to conclude that transferring more than 50% of the population from the level $|0\rangle$ to the level $|1\rangle$ is impossible using only a coherent control field.

Measurements performed on the system can break the dynamical symmetry thereby allowing for exceeding the above 50% population transfer limitation. Numerically, the measurement-assisted control problem for this system was investigated in Ref. [22], where transferring 66.9% of the population to the level $|1\rangle$ was obtained with a coherent control field assisted by a single measurement of P_0. In this section we analytically treat this control problem to find the upper bound on the maximal population transfer to the level $|1\rangle$, which is found to be approximately 68.7%. We also explicitly find the Rabi Frequencies of the optimal pulses, thus providing a complete analytical solution to this problem.

The control process consists of the following three steps. First, the system evolves under the action of a coherent field during the time interval $[0, t_1)$. Second, at the time $t = t_1$ a non-selective measurement of P_0 is performed on the system, which transforms the system state in accordance with the von Neumann scheme. Third, the system evolves during the time interval $(t_1, T]$ again only under the action of a coherent field.

Spontaneous emission during the first and third steps is neglected in this consideration. Therefore the system's dynamics under the action of an electromagnetic coherent field during the first and third steps can be described by optical Bloch's equation without relaxation terms:

$$\frac{d\rho(t)}{dt} = -i[H, \rho(t)]. \tag{40}$$

Here the Hamiltonian $H = \Omega(t)|0\rangle\langle 1| + \Omega(t)|1\rangle\langle 2| + \text{h.c.}$ is determined by the Rabi frequency $\Omega(t)$ of the electromagnetic field $\varepsilon(t)$. The symmetry of the system implies that the Rabi frequencies for the transitions $|0\rangle \leftrightarrow |1\rangle$ and $|1\rangle \leftrightarrow |2\rangle$ are the same.

Without loss of generality, it is sufficient to consider, constant Rabi frequencies during each step of the control. If the Rabi frequency Ω is time independent, then the Hamiltonian has the form $H \equiv H(\Omega) = \Omega|0\rangle\langle 1| + \Omega|1\rangle\langle 2| + \text{h.c.}$ and the solution of (40) with the initial condition $\rho(t_0) = \rho_0$ is $\rho(t) = U(t - t_0)\rho_0 U^\dagger(t - t_0)$, where $U(\tau) = e^{-i\tau H(\Omega)}$. The Hamiltonian $H(\Omega)$ can be written in terms of the vector $|\Omega\rangle = [\Omega|0\rangle + \Omega^*|2\rangle]/\sqrt{2}|\Omega|$ as $H(\Omega) = \sqrt{2}|\Omega|[|1\rangle\langle\Omega| + |\Omega\rangle\langle 1|]$ (here Ω^* is the complex conjugate of Ω). One has

$$\begin{cases} [H(\Omega)]^2 = 2|\Omega|^2[|1\rangle\langle 1| + |\Omega\rangle\langle\Omega|] \\ [H(\Omega)]^3 = 2|\Omega|^2 H \end{cases} \Rightarrow \begin{cases} [H(\Omega)]^{2n} = (\sqrt{2}|\Omega|)^{2n}[|1\rangle\langle 1| + |\Omega\rangle\langle\Omega|] \\ [H(\Omega)]^{2n+1} = (\sqrt{2}|\Omega|)^{2n+1}[|1\rangle\langle\Omega| + |\Omega\rangle\langle 1|] \end{cases}$$

This gives

$$U(\tau) = P_{\widetilde{\Omega}} + \cos\Big(\sqrt{2}|\Omega|\tau\Big)\Big(|1\rangle\langle 1| + |\Omega\rangle\langle\Omega|\Big) - i\sin\Big(\sqrt{2}|\Omega|\tau\Big)\Big(|1\rangle\langle\Omega| + |\Omega\rangle\langle 1|\Big) \tag{41}$$

where $P_{\widetilde{\Omega}} = \mathbb{I} - |1\rangle\langle 1| - |\Omega\rangle\langle\Omega| = |\widetilde{\Omega}\rangle\langle\widetilde{\Omega}|$ is the projector onto the subspace generated by the vector $|\widetilde{\Omega}\rangle = (\Omega|0\rangle - \Omega^*|2\rangle)/\sqrt{2}|\Omega|$.

In the first stage of control, the initial density matrix ρ_0 is transformed into $\rho_1 = U_1\rho_0 U_1^\dagger = |\psi_1\rangle\langle\psi_1|$, where $|\psi_1\rangle = U_1|0\rangle$ and $U_1 = \exp[-it_1 H(\Omega_1)]$ is the evolution operator induced by the control field with some Rabi frequency $\Omega_1 = |\Omega_1|e^{i\psi_1}$. Direct calculations give $|\psi_1\rangle = C_0|0\rangle + C_1|1\rangle + C_2|2\rangle$ with

$$C_0 = \frac{\cos\left(\sqrt{2}|\Omega_1|t_1\right) + 1}{2}, \qquad C_1 = \frac{i\sin\left(\sqrt{2}|\Omega_1|t_1\right)}{\sqrt{2}}e^{-i\psi_1}, \qquad C_2 = \frac{\cos\left(\sqrt{2}|\Omega_1|t_1\right) - 1}{2}e^{-2\psi_1}$$

Measuring the projector P_0 at the time $t = t_1$ transforms the pure state ρ_1 into the density matrix

$$\begin{aligned}\rho_2 = \mu_{P_0}(\rho_1) &= P_0\rho_1 P_0 + (\mathbb{I} - P_0)\rho_1(\mathbb{I} - P_0) \\ &= |C_0|^2 P_0 + |C_1|^2 P_1 + |C_2|^2 P_2 + C_1 C_2^* |1\rangle\langle 2| + C_1^* C_2 |2\rangle\langle 1|\end{aligned}$$

If $C_1 \neq 0$, then the state ρ_2 is mixed and the measurement destroys the coherence between the levels $|0\rangle$ and $|1\rangle$ while preserving the coherence between $|1\rangle$ and $|2\rangle$.

After the measurement the system density matrix evolves under action of a coherent field with some Rabi frequency $\Omega_2 = |\Omega_2|e^{i\psi_2}$ into $\rho_3 = U_2\rho_2 U_2^\dagger$. Here $U_2 = \exp[-it_2 H(\Omega_2)]$ is the evolution operator induced by the coherent field and $t_2 = T - t_1$. The density matrix $\rho_3 = U_2\left[\mu_{P_0}\left(U_1\rho_0 U_1^+\right)\right]U_2^\dagger$ can be computed using (41). The computation gives the following population $P = \langle 1|\rho_3|1\rangle$ of level $|1\rangle$ at the target time $t = T$,

$$P = \frac{1}{16}\Big\{5 - \cos(x_1) - [1 + 3\cos(x_1)]\cos(x_2) + 2[2\sin(x_1/2) - \sin(x_1)]\sin(x_2)\cos(\psi_2 - \psi_1)\Big\}, \tag{42}$$

where $x_1 = 2\sqrt{2}|\Omega_1|t_1$ and $x_2 = 2\sqrt{2}|\Omega_2|t_2$. This function is maximized by

$$x_1^* = \pm\left[2\arctan\left(\frac{\sqrt{18 + 2\sqrt{6}}}{\sqrt{6} - 1}\right) - 2\pi\right] \tag{43a}$$

$$x_2^* = \mp\arctan\left(\frac{\sqrt{18 + 2\sqrt{6}}}{\sqrt{6} - 1}\right) \tag{43b}$$

and by ψ_1, ψ_2 such that $\psi_2 - \psi_1 = 2\pi k$, $k = 0, \pm 1, \pm 2, \ldots$. The maximal value is

$$P_{\max} = \max_{\Omega_1,\Omega_2} P = 4 \cdot 10^{-3}\left(\sqrt{393 - 48\sqrt{6}} + 138 + 7\sqrt{6}\right) \approx 68.7\%. \tag{44}$$

This maximal population transfer to the level $|1\rangle$ can be obtained by applying a coherent field with Rabi frequency $\Omega_1 = x_1^*/(2\sqrt{2}t_1)e^{i\psi_1}$ to the system during the time interval $[0, t_1]$, then measuring the projector P_0 at time t_1, and finally applying a coherent field with Rabi frequency $\Omega_2 = x_2^*/(2\sqrt{2}t_2)e^{i\psi_2}$ during the time interval $[t_1, T]$, where $\psi_2 = \psi_1 + 2\pi k$, $k = 0, \pm 1, \pm 2, \ldots$.

Another simple way to compute the maximal yield is with the well-known Euler decomposition of the $SU(2)$ Lie group [37]. Suppose the system' propagation consists of the following

three steps:

$$\rho_1 = U_1^\dagger \rho_0 U_1 \tag{45a}$$

$$\rho_2 = \rho_1 - [P_k, [P_k, \rho_1]] \tag{45b}$$

$$\rho_3 = U_2^\dagger \rho_2 U_2 \tag{45c}$$

where Euler's decomposition of the unitary propagators is as follows:

$$U_k = \exp\left(i a_k H_0\right) \exp\left(i \frac{x_k}{2\sqrt{2}} \mu\right) \exp\left(i b_k H_0\right), \; k = 1, 2, \tag{46}$$

and $a_{1,2}, b_{1,2}$ and $x_{1,2}$ are six independent variables to be optimized with. Simple computation yields the population of the level $|1\rangle$ as

$$(\rho_3)_{11} = \frac{1}{16}\left[5 - \cos x_2 - \cos x_1 \left(1 + 3\cos x_2\right) + 2\cos\left(a_2 + b_1\right)\left(\sin x_1 - 2\sin\frac{x_1}{2}\right)\sin x_2\right], \tag{47}$$

with which it is easy to derive the same maximal population transfer shown in Eq. (44).

VI. CONCLUSION

This paper discusses the use of both instantaneous and continuous observations in the manipulation of quantum dynamics. The measurements can be viewed as direct controls. Two-level systems and a special three-level system are treated analytically. Solutions and upper bounds for the controlled processes are obtained, and they agree very well with previous numerical simulations, and QAZE is recovered. The results are proper for instantaneous observations performed any number of times and continuous observations performed with any strength. The performance of optimal observations hopefully will become routine with advancing technology, as observations can be powerful tools in the control of quantum dynamics.

Acknowledgments

The authors acknowledge support from the NSF and an ARO grant.

[1] S. A. Rice and M. Zhao, *Optical Control of Molecular Dynamics* (Wiley, New York, 2000).

[2] H. Rabitz, R. de Vivie-Riedle, M. Motzkus, and K. Kompa, Science **288**, 824 (2000).

[3] H. Rabitz, Theor. Chem. Acc. **109**, 64 (2003).

[4] M. Shapiro and P. Brumer, *Principles of the Quantum Control of Molecular Processes* (John Wiley, New York, 2003).

[5] V. Bonacic-Koutecky and R. Mitric, Chem. Rev. **105**, 11 (2005), URL http://dx.doi.org/10.1021/cr0206925.

[6] D. D'Alessandro, *Introduction to Quantum Control and Dynamics* (Chapman and Hall, Boca Raton, 2007).

[7] I. Walmsley and H. Rabitz, Phys. Today **56**, 43 (2003).

[8] T. Brixner, N. H. Damrauer, and G. Gerber, in *Advances in Atomic, Molecular, and Optical Physics*, edited by B. Bederson and H. Walther (Academic, San Diego, CA, 2001), vol. 46, pp. 1–54.

[9] M. Dantus and V. Lozovoy, Chem. Rev. **104**, 1813 (2004), URL http://dx.doi.org/10.1021/cr020668r.

[10] W. Zhu and H. Rabitz, J. Chem. Phys. **118**, 6751 (2003), URL http://link.aip.org/link/?JCP/118/6751/1.

[11] F. Shuang and H. Rabitz, J. Chem. Phys. **121**, 9270 (2004), URL http://link.aip.org/link/?JCP/121/9270/1.

[12] F. Shuang and H. Rabitz, J. Chem. Phys. **124**, 154105 (2006), URL http://link.aip.org/link/?JCP/124/154105/1.

[13] F. Shuang, H. Rabitz, and M. Dykman, Phys. Rev. E **75**, 021103 (2007), URL http://link.aps.org/abstract/PRE/v75/e021103.

[14] A. Pechen and H. Rabitz, Phys. Rev. A **73**, 062102 (2006), URL http://dx.doi.org/10.1103/PhysRevA.73.062102; arXiv:quant-ph/0609097.

[15] A. Pechen and H. Rabitz, arXiv:0801.3467 [quant-ph] (2008).

[16] R. S. Judson and H. Rabitz, Phys. Rev. Lett. **68**, 1500 (1992).

[17] L. Roa, A. Delgado, M. L. Ladron de Guevara, and A. B. Klimov, Phys. Rev. A **73**, 012322 (2006).

[18] R. Vilela Mendes and V. I. Man'ko, Phys. Rev. A **67**, 053404 (2003).

[19] J. Gong and S. A. Rice, J. Chem. Phys. **120**, 9984 (2004).

[20] M. Sugawara, J. Chem. Phys. **123**, 204115 (2005).

[21] M. Sugawara, Chem. Phys. Lett **428**, 457 (2006).

[22] F. Shuang, A. Pechen, T.-S. Ho, and H. Rabitz, J. Chem. Phys. **126**, 134303 (2007), URL `http://link.aip.org/link/?JCP/126/134303/1`; `arXiv:quant-ph/0609084`.

[23] A. Pechen, N. Il'in, F. Shuang, and H. Rabitz, Phys. Rev. A **74**, 052102 (2006), URL `http://dx.doi.org/10.1103/PhysRevA.74.052102`; `arXiv:quant-ph/0606187`.

[24] M. B. Mensky, *Continuous Quantum Measurements and Path Integrals* (IOP, Bristol, 1993).

[25] V. Neumann, *Mathematical Foundations of Quantum Mechanics* (Princeton University Press, Princeton, 1955).

[26] M. Mensky, Phys. Lett. A **196**, 159 (1994).

[27] D. F. Walls and G. J. Milburn, *Quantum Optics* (Springer, Berlin, 1994).

[28] B. Misra and E. Sudarshan, J. Math. Phys. **18**, 756 (1977).

[29] W. M. Itano, D. J. Heinzen, J. J. Bollinger, and D. J. Wineland, Phys. Rev. A **41**, 2295 (1990).

[30] A. P. Balachandran and S. M. Roy, Phys. Rev. Lett. **84**, 4019 (2000).

[31] A. Roberts and D. Varberg, *Convex Functions* (Academic Press, New York, 1973).

[32] N. Hansen and A. Ostermeier, Evol. Comput. **9**, 159 (2001).

[33] N. Hansen and S. Kern, in *Parallel Problem Solving from Nature - PPSN V* (Springer, Amsterdam, 1998), vol. 1498 of *Lecture Notes in Computer Science*, pp. 282–291.

[34] A. Auger and N. Hansen, in *Proceedings of the IEEE Congress on Evolutionary Computation*, edited by D. C. et al (IEEE Press, Piscataway, NJ, USA, 2005), pp. 1777–1784.

[35] O. M. Shir, C. Siedschlag, T. Bäck, and M. J. Vrakking, in *2006 IEEE World Congress on Computational Intelligence*, edited by S. M. Lucas and et al (IEEE Computational Intelligence Society, 2006), pp. 9817–9824.

[36] G. Turinici and H. Rabitz, Chem. Phys. **267**, 1 (2001).

[37] L. C. Biedenharn and J. D. Louck, *Angular Momentum in Quantum Physics*, vol. 8 of *Encyclopedia of Mathematics and its Applications* (Addison-Wesley Publishing Co., Reading, Mass., 1981).

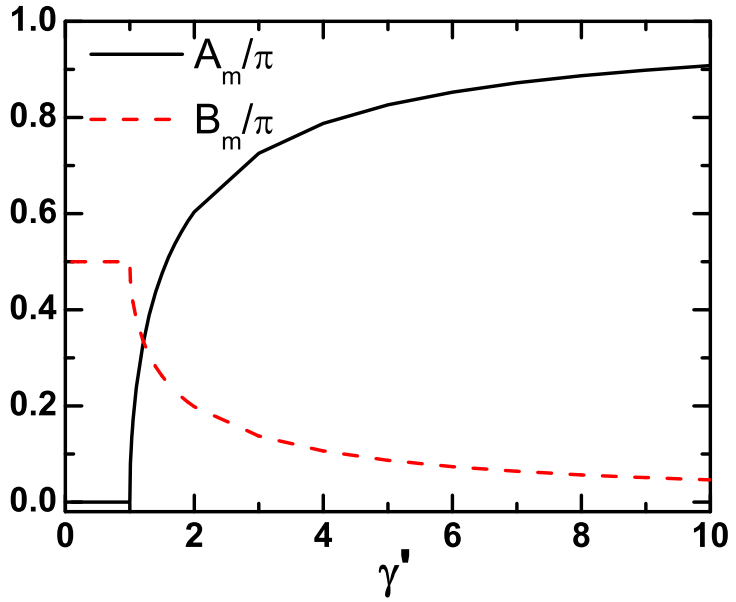

Fig. 1

FIG. 1: (Color online) Optimal coefficients A_m and B_m of the linear function $\alpha(t)$ in the projection operators (ref. Eq. (21a)) which are continuously measured to control the quantum dynamics of a two-level system. In the optimization process, the functions $\alpha(t)$ and $\theta(t)$ in the projection operators are assumed to be linear and zero, respectively, and the optimal solutions are proved to be globally optimal. γ' (dimensionless) is multiplication of observation strength and observation time (ref. Eq. (25a)).

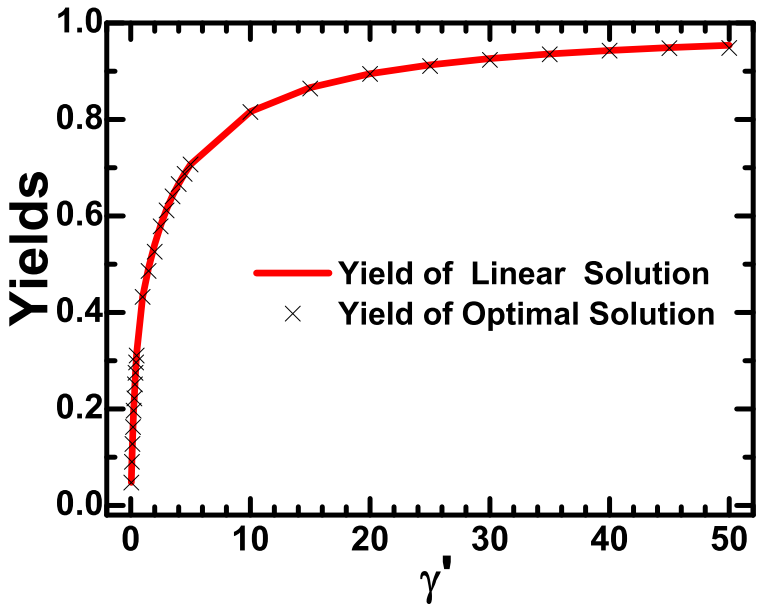

Fig. 2

FIG. 2: (Color online) The yield as a function of the observation strength for the linear solution (solid line), with the best attained yield with an evolutionary search using the CMA-ES algorithm (squares) as a reference. The latter non-linear solutions did not exceed the linear solution's global optimal yield. γ' (dimensionless) is multiplication of observation strength and observation time (ref. Eq. (25a)).